JOURNAL OF GEOPHYSICAL RESEARCH, VOL. 106, NO. D17, PAGES 20,395–20,402, SEPTEMBER 16, 2001

Theory of charge and mass transfer in ice-ice collisions

J. G. Dash
Department of Physics, University of Washington, Seattle, Washington

B. L. Mason
Stanford Research Systems, Sunnyvale, California

J. S. Wettlaufer
Department of Physics and Applied Physics Laboratory, University of Washington, Seattle, Washington

Abstract. A new model describes charge and mass transfer in ice-ice collisions in terms of fundamental molecular physics. Drawing on clues from results of recent and earlier experiments, the theory treats the collisions as interlinked events acting in three stages: before collision, during contact, and withdrawal. The theory provides quantitative descriptions of charge and mass transfer and their dependence on growth rate, temperature, and impact energy. Application of the theory to experimental simulations of thunderstorm charging explains general trends in terms of basic microscopic processes.

1. Introduction

Laboratory studies have shown that collisional charging of ice particles can account for the observed electric fields in thunderstorms [*Reynolds et al.*, 1957; *Latham and Stow*, 1965; *Buser and Aufdermaur*, 1977; *Takahashi*, 1969, 1978; *Gaskell and Illingworth*, 1980; *Jayaratne et al*, 1983; *Baker et al.*, 1987; *Keith and Saunders*, 1990; *Caranti et al.*, 1991; *Saunders et al.*, 1991; *Avila et al.*, 1996; *Brooks et al.*, 1997; *Saunders and Peck*, 1998; *Jayaratne*, 1998]. Several theories have been proposed to model the microphysical process, but they have had limited success in describing the phenomena. Recently, a novel experiment [*Mason and Dash*, 1999, 2000] (hereinafter referred to as MD), which was designed to test the predictions of a model proposed by *Baker and Dash* [1989, 1994], has provided additional clues. These results, together with the earlier work, have led us to develop a new model of the basic charging mechanism. The principal features that the theory captures are as follows: (1) Particles experiencing more rapid vapor growth charge positively. (2) Positive charging is due to the loss of negative charge. (3) Charging is proportional to growth rate at low rates but increases more slowly with growth at high rates. (4) Charge transfer is enhanced by surface disorder. (5) Liquid-like mass transfer accompanies charging, with the colder particle gaining mass. These features form the basic observations of the MD experiment and are found in many of the previous studies. The theory is first outlined and then described in detail. The model is successfully tested against the measurements of the MD study. It is then applied to other collisional charging studies, where it explains some of the principal trends in terms of basic molecular processes.

2. Outline of the Theory

Rapid vapor deposition can produce disordered growth, with ionic defects at vapor and grain boundary interfaces, at densities increasing with growth rate. The OH^- ions are bound to sites by their remaining hydrogen bonds, while positive ions diffuse more readily away from the surface into the ice, thereby creating a charged double layer and a negative surface potential. When two vapor-grown ice particles collide, they tend to equalize their surface charge densities, thus causing the more rapidly grown particle to lose negative charge. The charge transfer is enhanced by collisional melting, whereby the outer layers of the particles are temporarily liquified, to depths proportional to the impact energy. The melting allows the outer, negative charge regions to diffuse and equalize rapidly in the melted layer, while the deeper positive charges cannot escape from the ice during the brief time of collision. On disengagement, the particles tend to take roughly equal portions of the liquid. Systematics of mass and charge transfer in low- and high-impact collisions are described quantitatively.

Paper number 2001JD900109.
0148-0227/01/2001JD900109$09.00

3. Theoretical Details

3.1. Before Contact

Solids growing rapidly by vapor deposition have rough surfaces and internal defects owing to the limited rate at which molecules diffuse to crystal steps where they can be incorporated into the lattice. The phenomenon has been demonstrated by computer simulations [*Stolze and Norskov*, 1993; *Smith and Srolovitz*, 1996] and laboratory experiments on metals [*Krim and Palasantzas*, 1995] and ice [*Kouchi et al.*, 1994].

The scale of disorder is set by a competition between the rate of surface diffusion between steps and the vapor flux. If the surface diffusion coefficient is D_s, then during a time $\mathcal{T}$ a surface molecule travels a distance $\lambda = (2D_s\,\mathcal{T})^{1/2}$ [*Einstein*, 1905] before being buried by other molecules from the vapor. The time $\mathcal{T}$ is related to the flux F by $\mathcal{T} = (AF)^{-1}$, where A is the area of a surface site. Thus the typical distance between steps and other defects is

$$\lambda = \sqrt{2D_s/AF}\ . \qquad (1)$$

With $D_s = 1.5 \times 10^{-13}$ m^2 s^{-1} [*Mizuno and Hanafusa*, 1987] and AF ranging from 20–120 s^{-1} (MD), we have $\lambda = 120$–50 nm.

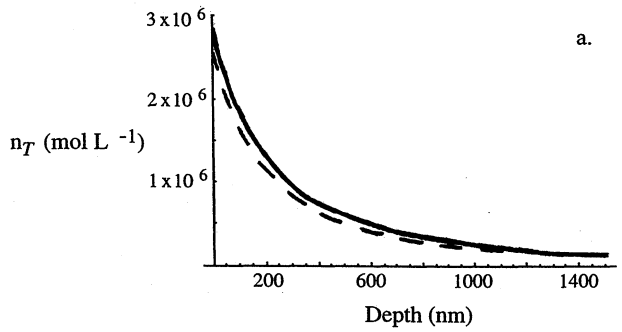

Figure 1a. Profiles of the net positive charge distribution n_T in a growing ice crystal; $n_T = n_+ - n_-$. The surface is located at a depth of zero. The negative charge, which is not shown, is localized at the surface. The curves are derived from Gouy-Chapman theory (equation (6)) for a surface charge density comparable to that of the *Mason and Dash* [1999, 2000] experiments at temperatures between –20°C and –5°C. To encompass the possible range of growth-induced disorder, the values of background ion densities n_b are set between bulk water and bulk ice. Here $\sigma_g = 10^{-4}$ C m^{-2}, the Mason and Dash estimate, and the solid (dashed) curve is for a backgroud density $n_b = 1.7 \times 10^{-7}$ mol L^{-1} (1.7×10^{-11} mol L^{-1}). It is seen that the variation of background ion densities of 4 orders of magnitude has little quantitative influence on the detailed depth profiles.

Bond disorder and ionization exist in bulk ice [*Eigen and De Maeyer*, 1958; *Onsager and Dupuis*, 1959], in greater density at crystal surfaces [*Dosch et al.*, 1995, 1996], and even more at defects and rough surfaces [*Mae and Higash*, 1973]. On prismatic facets the equilibrium density of hydrogen bond disorder is $\rho_B = 5.7 \times 10^{25}$ m^{-3} averaged over a depth of 20 to 25 nm [*Dosch et al.*, 1995, 1996]. The bond disorder implies a certain density of ionic defects: the ratio of ionic to bond defects is $\rho_i / \rho_B \approx 10^{-5}$ in bulk ice near the melting point [*Onsager and Dupuis*, 1959]. This leads to an estimate of the integrated surface density of ionization of an equilibrium prism facet of $\sigma_s \approx 2 \times 10^{-6}$ C m^{-2}.

Additional ionization occurs at rough and damaged surfaces owing to the reduced bonding at crystal edges and corners. The ionization into OH^- and H^+ tends to develop into a negative surface layer and a diffuse positive distribution deeper in the ice. The localization of the OH^- ion is due to its binding to the neighboring molecules by its remaining hydrogen bond, while the positive ions diffuse owing to their high mobility [*Engelhardt*, 1973; *Pines and Huppert*, 1985] and the availability of a large configuration volume in the bulk ice. This polarity is consistent with measurements of surface potential, which show that surface damage or riming can produce a negative value of several hundred millivolts [*Caranti and Illingworth*, 1983].

According to the foregoing, the disorder-induced ionization is proportional to the density of surface growth defects. By (1) we have

$$\sigma_g \approx e/\lambda^2 = \xi eAF/2D_s \qquad (2)$$

where e is the elementary charge. The parameter ξ is defined as the surface structural disorder factor, which may depend on conditions such as atmospheric impurities and age and temperature history. At this stage, ξ is treated as a fitting parameter, and it is the only adjustable parameter in the theory.

The development of a diffuse positive ion distribution in the ice is similar to that of counterions liberated from an ionized surface in water [*Verwey and Overbeek*, 1948; *Israelachvili*, 1992]. An analogy is the formation of a vapor atmosphere above an evaporating source in a gravitational field. The diffusion of the vapor is driven by the particle kinetic energy, while its altitude is limited by gravity. This competition produces an exponential density distribution, with a scale length determined by temperature and gravitational potential. In the charged double layer the potential energy is electrostatic, and the characteristic distance is termed the Debye length. For an isolated planar surface of charge density σ_s, the electric field is independent of distance: $E = \sigma_s / 2\varepsilon\varepsilon_o$, where ε is the dielectric constant of the

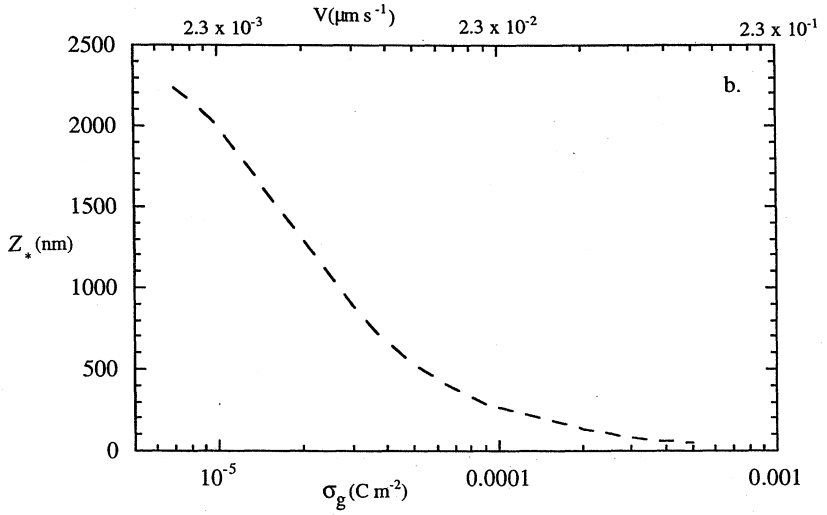

Figure 1b. Effect of the internal field between the positive and negative ion distributions, in which larger charge densities tend to localize the positive ions closer to the interface. A semilog plot of the depth Z_* at which the net ion density n_T reaches $1/e$, the interfacial value n_T ($z = 0$), is shown as a function of the ice growth rate V (μm s^{-1}) and the surface charge density σ_g as determined from equation (2). The bulk density is 1.7×10^{-8} mol L^{-1}. The range of the *Mason and Dash* [1999, 2000] study is 1.67×10^{-3} to 3.3×10^{-2} μm s^{-1}.

medium and ε_o is the vacuum permittivity. When the contact potential is negative, the surface field is screened by positive counterions. If there is a finite background density of ions, their screening will compress the distribution, i.e., reduce their average distance from the surface.

For arbitrary contact potential ψ_s the form of the ion distribution is described by the electrostatic potential energy:

$$\psi(z) = \frac{2k_bT}{e} \ell n \left[\frac{1 + tanh\left(\frac{e\psi_s}{4k_bT}\right) e^{-\kappa z}}{1 - tanh\left(\frac{e\psi_s}{4k_bT}\right) e^{-\kappa z}} \right], \quad (3)$$

where z measures the distance from the surface into the bulk and κ^{-1} is the Debye length, given by

$$\kappa^{-1} = \left(\frac{\varepsilon\varepsilon_o k_b T}{e^2 n_{b_\pm}} \right)^{1/2}, \quad (4)$$

where $n_{b\pm}$ is the background ion density of cations (n_{b+}) or anions (n_{b-}) in the bulk and k_b is Boltzmann's constant [see, e.g., *Verwey and Overbeek*, 1948; *Israelachvili*, 1992]. The contact potential is written in terms of the surface charge density as

$$\psi_s = \frac{2k_bT}{e} sinh^{-1}\left(\frac{\sigma_s}{\sqrt{8\varepsilon\varepsilon_o k_b T n_{b_\pm}}} \right). \quad (5)$$

The potential described by (3) yields the counterion and coion densities through the Boltzmann distribution

$$n_\pm(z) = n_{b_\pm} e^{\pm \frac{e\psi(z)}{k_bT}}. \quad (6)$$

The influence of growth can be incorporated by relating the static surface charge density in (5) to that of (2): $\sigma_s \rightarrow \sigma_s + \sigma_g$. In Figures 1a and 1b the calculated net charge distribution and its dependence on growth rate are shown for experimental conditions.

3.2. During Contact: Collisional Melting

Surface and interfacial premelting are well-known phenomena [*Nenow and Trayanov*, 1989; *Löwen*, 1994; *Frenken and van Pinxteren*, 1994; *Dash et al.*, 1995; *Oxtoby*, 1999]. The phenomena arise from the weaker bonding of a solid at its interface with vapor (surface melting) or a foreign solid (interfacial melting). This causes the outer layers to disorder more readily as temperature rises toward the bulk melting point. Surface melting has been observed on at least one crystallographic facet in virtually all materials, including metals, semiconductors, rare gas and organic solids, and ice. The equilibrium thickness of the melt layer depends on the temperature and the molecular interactions between the components of the system. For materials controlled by dispersion forces, the thickness d is given by

$$d = \left(-\frac{2\bar{\sigma}^2 \Delta\gamma}{\rho_\ell q_m t} \right)^{1/3}, \quad (7)$$

where q_m is the latent heat of fusion, $\bar{\sigma}$ is a length of the order of a molecular distance, ρ_ℓ is the molecular density of the liquid, $t = (T_m - T)/T_m$ is the reduced temperature, and T_m is the normal melting point of the bulk material. Exemplary cases of solids controlled by dispersion forces are Ar and Ne, where surface melting of the outermost layers begins above ~0.8 of the absolute temperature of bulk melting. The rate of increase of the liquid thickness is slow until very close to the transition. For example, at a reduced temperature, t = 0.99, the thickness of surface melting in argon is only 10 molecular layers [*Zhu and Dash*, 1986].

When the surface interactions are short ranged, the thickness relation is logarithmic:

$$d = d_o \ell n\left(-\frac{a_o \Delta\gamma}{\rho_\ell q_m t} \right), \quad (8)$$

where d_o and a_o are constants. Other interactions, such as electrostatic forces, can produce other similarly specific temperature dependences [*Wettlaufer et al.*, 1996].

Disorder in the neighborhood of the solid surface enhances premelting, by raising the local free energy of the solid relative to that of the liquid. Several possible forms of disorder can produce such an effect: roughness, polycrystallinity, strains and dislocations, and impurities [*Pengra et al.*, 1991; *Beaglehole and Wilson*, 1994; *Netz and Andelman*, 1997; *Wettlaufer*, 1999]. Whatever the type of disorder, its effect on surface melting can be described in terms of an increase of local energy density $\Delta\varepsilon$. For dispersion forces the thickness relation is changed from (7) to

$$d = \left(-\frac{2\bar{\sigma}^2 \Delta\gamma}{\rho_\ell q_m t - \Delta\varepsilon} \right)^{1/3}. \quad (9)$$

For short-range forces the perturbed thickness is

$$d = d_o \ell n\left(-\frac{a_o \Delta\gamma}{\rho_\ell q_m t - \Delta\varepsilon} \right). \quad (10)$$

Finally, if the region also contains a concentration c of impurities, the thickness of the melted layer is increased further: (7) develops into

$$d = \left(-\frac{2\bar{\sigma}^2 \Delta\gamma}{\rho_\ell q_m t - \Delta\varepsilon - ck_bT} \right)^{1/3}, \quad (11)$$

and the argument for short-range forces is similarly extended.

In applying the extended theory to ice, we note that surface melting is much weaker than is typical of other materials, most studies finding that equilibrium melting at ice–vapor interfaces does not exist below ~−4°C [*Beaglehole and Nason*, 1980; *Furukawa et al.*, 1987; *Elbaum et al.*, 1993]. At higher temperatures the measurements show considerable variation in thickness, owing to an extreme sensitivity to perturbations. In these circumstances the introduction of crystalline disorder, e.g., by collisional damage, can cause melting considerably more important than the equilibrium effect.

The expressions for d depend on $\Delta\varepsilon$ which is itself a function of the thickness. If the total damage energy ΔE is uniform over an area A to a depth d, then $\Delta\varepsilon = \Delta E/Ad$, and the simultaneous solution with (9) or (10) can be obtained graphically. Figure 2 illustrates solutions for dispersion forces, for different temperatures and damage energy. The intersections are extremely close to the divergent limit, hence the solution is very nearly

$$d_m = \frac{\Delta E}{A q_m t}. \quad (12)$$

Short-range and other power law interactions diverge at the same point, hence the form of d_m is approximately the same for all.

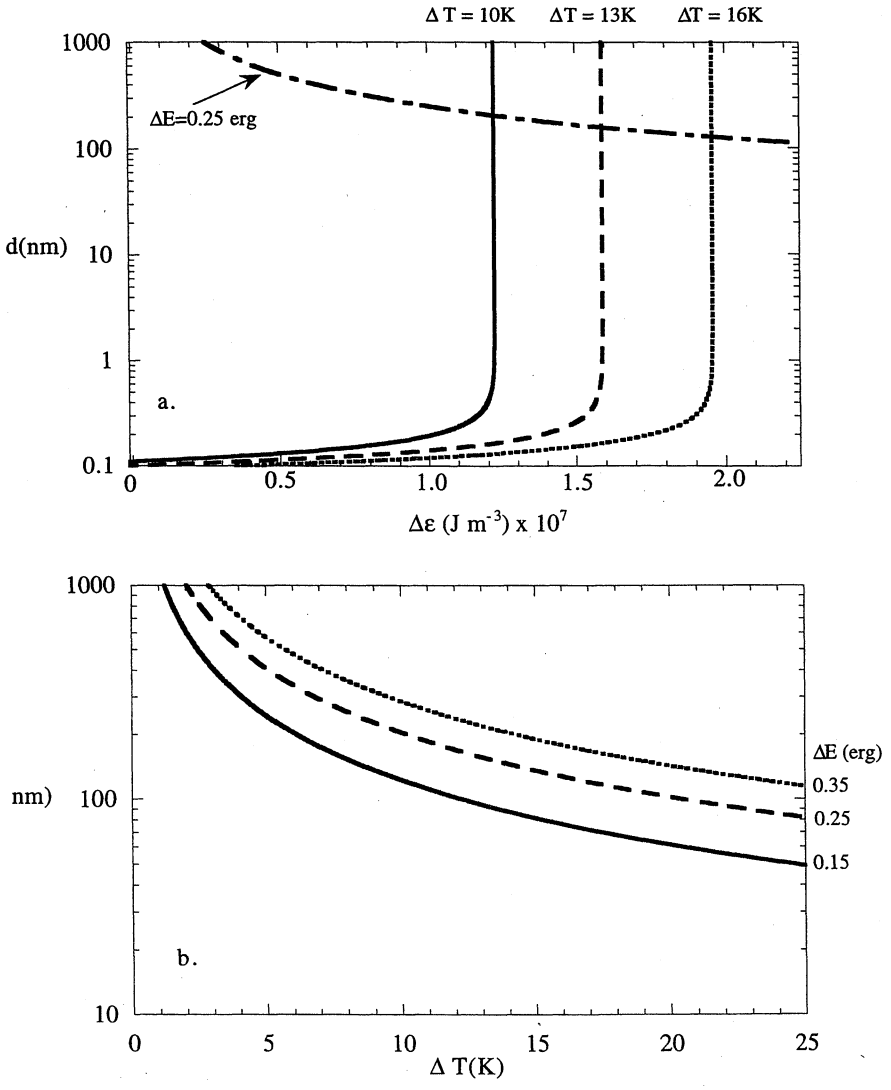

Figure 2. Damage assisted interfacial melting. (a) Theoretical film thickness versus damage energy per unit volume $\Delta\varepsilon$ at three temperatures. The curves are plotted as film thickness versus $\Delta\varepsilon$ at fixed total damage energy $\Delta\varepsilon = 2.5 \times 10^{-8}$ J, a value in the midrange of the experimental collisions in the *Mason and Dash* [1999, 2000] study. The intersections of these curves give the film thickness at that undercooling. (b) Film thickness d versus undercooling ΔT at various total damage energies ΔE. A difference of film thickness of ~40 nm occurs at a temperature difference of 3 K.

Melting during a collision allows the rapid diffusion of ions through the liquid layer. The diffusion coefficient of the ions in the melt layer is estimated to be of the order of 10^{-9} m^2 s^{-1}, comparable to the self-diffusion coefficient of liquid water near 0°C [*Eigen and De Maeyer*, 1958]. This value allows equalization of the charge distributions through a 40-nm-thick film to occur in a time of the order of a microsecond, well within the estimated 0.1 ms time of contact in the MD study. In contrast, the collision is too fast for most of the protons, which lie much deeper in the ice, to dissolve, for according to the proton diffusion coefficient in ice at −10°C [*Engelhardt*, 1973; *Pines and Huppert*, 1985], diffusion from a depth of 1 μm takes ~1 ms.

3.3. Disengagement

Mass transfer occurs when the particle temperatures are different; both melting and refreezing are asymmetric. The warmer particle, which in the MD experiments is subliming, has a thicker, interfacially melted film. Hence, when the particles separate, carrying away equal average thicknesses of film, the colder particle has a portion of the warmer particle's mass. If refreezing begins while the particles are still in contact, the colder particle captures an even larger fraction of the shared liquid film.

To quantify the effect of asymmetry in melting and compare it to the MD results, we note that a typical impact was estimated to deposit 5×10^{-8} J on a contact area of 10^{-8} m^2, resulting in a mass transfer of the order of a 30-nm-thick film. The actual temperature difference was not measured in the experiment, but at a mean temperature of −11°C it was estimated from the measured growth rates as ~1 K. The theory predicts that a melting point of −12.5°C would be produced if half of the estimated impact energy were deposited uniformly to a depth of ~161 nm. At a temperature 3 K higher, d is 218 nm; the difference amounts to ~57 nm. Approximately one half of this difference will be transferred during the disengagement, in agreement with the experimental mass transfer of about a 30-nm-thick film.

According to (2) and the measured surface diffusion coefficient [*Mizuno and Hanafusa*, 1987], the charge density on a surface growing at 30 nm s^{-1} is approximately equal to 1.4 x 10^{-4}C m^{-2}. This value is comparable to the measured charge transfer in a typical collision. Figure 3 shows the comparison of the theory with the measured charge transfer.

The estimates above assume that refreezing does not overtake the growing surface melted film. We estimate the amount of liquified material δh that can refreeze during the collision time $\delta\tau$ under the thermal conditions of the experiment as

$$\delta h \approx \frac{\delta\tau}{\rho_s q_m} k_i \nabla T \ , \qquad (13)$$

where k_i is the thermal conductivity of the ice and ∇T is an estimate of the local temperature gradient. A conservative estimate of the latter finds that for $\delta\tau$ between 0.1 and 1 ms, δh ranges from tens to hundreds of monolayers. Thus only a small fraction of the total melted layer refreezes before disengagement.

It is clear from Figure 3 that theory and experiment agree that the derivative of charge transfer with growth tends to saturate and then decrease at high growth rate and large impact energy. The decline results from compression of the charge distribution at high growth rate: the increased electrostatic field between the positive and negative charge distributions reduces their separation. Higher growth rate increases the charge density σ_g, inhibiting the diffusion of the cations, so that they do not penetrate the ice as deeply, as seen in Figure 1b. If the collision damage is great enough, it will expose a greater fraction of the positive ions to the subsequent melting, and when these are liberated into the melt, they neutralize a fraction of the anions. The saturation effect is a natural consequence of the theory. We did not address it during the development of the model and only discovered it as welcome supporting evidence when quantitative estimates were being made. The effect is mainly limited to the rather energetic collisions in the MD study; in typical charging studies the collisional melting does not invade deeply into the positive region (see section 4).

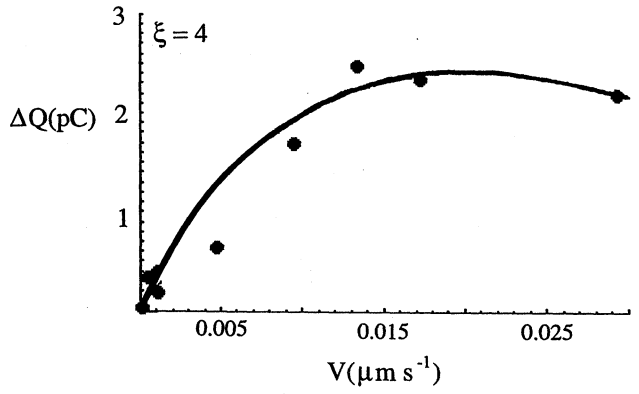

Figure 3. Charge transfer versus growth rate calculated from the theory, compared with *Mason and Dash* [1999, 2000] data. Here ΔQ is the charge over the collision area (10^{-8} m^{-2}) of the experiment gained by the growing particle versus the growth rate over a range spanning the Mason and Dash study. The theoretical curve is calculated with the experimental values of impact energy, collision area, and mean temperature, and a temperature difference of 3 K, greater than the 1 K estimated in the experiment. The surface structural disorder factor ξ = 4 yields the best fit overall. The saturation is driven by the neutralization provided by the dissolved cations. As more material participates in the collision, less negative charge is lost to the evaporating surface, and for a given total depth of shared melt liquid, the net negative charge loss decreases as the bulk ion density increases.

4. Application of the Theory to Charging in Thunderstorms

Previous sections of this paper describe how the theory was developed primarily on the basis of clues from the MD study, although it was constrained to be consistent with the general findings of earlier work. In this section we compare the model with results of other studies of ice collisions designed to model the more complex charging conditions in natural thunderstorms.

These experiments, which involve collisions between small ice particles and large ice-covered targets (graupel), typically show a reversal of charge transfer polarity at various temperatures, collision speeds, and liquid water content of the atmosphere. *Baker et al.* [1987] proposed the principle that the particle growing more rapidly from the vapor charges positively as a result of a collision, and several subsequent studies [*Saunders*, 1994; *Jayaratne et al.*, 1996; *Avila et al.*, 1996; *Jayaratne*, 1998; *Saunders and Peck*, 1998] obtained results in substantial agreement. The present theory provides an explanation in terms of the molecular dynamics of vapor growth, whereby crystal disorder results from the limited rate at which depositing molecules can be incorporated into a smooth crystal facet. The disorder creates a population of molecules with broken bonds, which ionize and form a charged double layer with a negative surface charge and a deeper, diffuse positive charge. This polarity results from the pinning of the OH^- ion to its site by the remaining hydrogen bond, while the diffusion of the proton is due to its mobility and the large number of states available in the volume of the crystal.

The surface charge per unit area on each particle is therefore proportional to the vapor flux, i.e., to the vapor growth rate of the particle. If two particles have different vapor growth rates, the particle growing more rapidly has a greater negative surface charge density. Brief contact between two surfaces carrying different charge densities will allow charge transfer, if the charge carriers are sufficiently mobile. The double layer as a whole is electrically neutral, hence the net charge transfer must involve a difference between the rate of transfer of the positive and negative distributions. During growth the surface OH^- ions are localized by site forces and can be dislodged only when the local fields are sufficiently high. However, the site localization disappears on melting, so that the surface ions can diffuse and mix in the liquid during the time of contact. In contrast, the positive ions are distributed over a depth in the solid, diffuse more slowly, and are mostly retained during the collision. Therefore melting during the contact should be a significant factor in the magnitude of charge transfer. It is treated in detail in section 3.2 and summarized in the next paragraph.

Surface melting is a phenomenon displayed by virtually all materials, whereby the solid develops a liquid-like surface layer below the bulk melting temperature T_m. The effect has been intensely studied and is well understood thermodynamically and on the molecular level. There have been several reviews; two that have treated surface melting specifically in ice are by *Nenow and Trayanov* [1989] and *Dash et al.* [1995]. Interfacial and grain boundary melting are varieties of surface melting, occurring at the interfaces with foreign materials and between crystals of the same material. All are enhanced by damage or other sources

of crystal disorder, lowering the starting temperature and increasing the thickness of the melt layer. A quantitative theory of the enhancement, here termed collisional melting, is developed in section 3.2.

The thickness of the collisionally melted liquid can be calculated with (12). The contact area A can be estimated according to the Hertzian theory of elastic collision between a sphere and a plane [*Tabor*, 1951; *Gaskell and Illingworth*, 1980; *Pittenger et al.*, 1998]:

$$A = 13.4 V^{4/5} R^2 \left(\rho / E_e\right)^{2/5} (\cos\phi)^2, \qquad (14)$$

where R is the sphere radius, E_e is the effective Young's modulus, V is the speed, and ϕ is the angle of impact.

The effective modulus for dissimilar materials depends on the individual moduli E_1 and E_2 and Poisson's ratios ν_1 and ν_2, according to

$$1/E_e = \left(1-\nu_1^2\right)/E_1 + \left(1-\nu_2^2\right)/E_2. \qquad (15)$$

For ice at –5°C, E = 9.4 GPa, ν = 0.33 [*Fletcher*, 1970], hence E_e = 5.3 GPa.

The calculation of melting depth requires an estimate of the energy loss in a typical rebounding collision. Although there are several measurements of collision efficiency of water droplets [see, e.g., *Qian and Law*, 1997] and ice spheres [see, e.g., *Arakawa and Higa*, 1996], we find no measurements or theories specifically appropriate to the range of sizes and velocities of ice-ice collisions in the charging studies. According to the papers cited, the fractional loss varies with all of the parameters of the collision, namely, the particle size, energy, and impact angle. In addition, we expect that the collisional melting phenomenon itself will introduce a variation with temperature. In this situation one has only an upper bound for ΔE, which, allowing for the rebound, is nearly equal to all of the incoming energy. However, for the purpose of illustration, we will assume that the loss is only 10% of the initial kinetic energy. With this estimate the calculations below predict appreciable collisional melting in the range of the experiments. Larger collisional losses will, of course, produce greater depths.

The depths d_m are given in units of molecular layers: (1) R = 10 μm, V = 1 m s^{-1}, T = –35°C, $d_m \approx 6$; (2) R = 25 μm, V = 3 m s^{-1}, T = –15°C, $d_m \approx 40$; (3) R = 50 μm, V = 10 m s^{-1}, T = –5°C, $d_m \approx 500$.

In addition to the energy loss, the calculations are subject to several corrections and uncertainties. The estimates are for a well-ordered ice crystal, whereas the kinetic roughening will cause changes in all of the properties, and the collisional melting itself causes a reduction of the effective elastic modulus. An important effect of the melting is the local plasticity of the surface, which allows greater areas of contact, affording greater possible charge exchange.

A quantitative estimate of the charge transfer in typical collisional charging experiments is more problematical. In most of these studies a cloud of ice particles falls in an atmosphere of supercooled water droplets, while an ice-covered target sweeps through the cloud. The growth rate of the particles depends on the temperature and concentration of the water droplets, while the vapor growth of the target is primarily due to riming. Detailed calculations by *Baker et al.* [1987] show that the vapor that emanates during the freezing of riming water droplets is primarily deposited on the nearby ice surface. The target's growth therefore depends on its speed, collection efficiency, and temperature as well as the temperature and density of the supercooled water droplets. The dependence of charge transfer on these variables has been further developed in many subsequent studies [*Keith and Saunders*, 1990; *Caranti et al.*, 1991; *Saunders et al.*, 1991; *Avila et al.*, 1996; *Brooks et al.*, 1997; *Saunders and Peck*, 1998; *Jayaratne*, 1996, 1998], and functional equations have been fitted to the data over limited regimes. *Keith and Saunders* [1990] showed that the charge transfer to the target depended on crystal size and speed as power laws, with exponents varying over particular ranges of size and temperature in the positive and negative charging regimes. The data were extended and further analyzed by *Saunders et al.* [1991]. For example, in the negative charging regime, over the size range 10–450 μm the exponent for size ranged from 2.5 to 1.9, while the speed exponent was constant at 2.5.

On the basis of the present theory, we expect a variation with size primarily through the collision area, i.e., quadratically. The velocity exponent would be 1.8, owing to the combination of target speed and the collision area. Additional dependence on V and R should arise from collisional melting, which changes the elasticity of the surface and hence the area of impact.

The dependence of charge transfer magnitude on temperature can be especially complicated, since temperature affects both the collisional melting and the evaporation rate of the supercooled droplets. In view of these complications we do not attempt to develop a more quantitative application of the theory to collisional charging as observed in experiments other than those in MD. However, we note an intriguing temperature dependence predicted by the theory, owing to a decrease of the collisional melting thickness at lower temperature, which should cause a corresponding decrease in the magnitude of charge transfer in collisions. For the smallest particles and lowest speeds of typical experiments, there will be very little melting below about ~–40°C. Experiments and thundercloud temperatures indicate comparable limits to charge transfer.

5. Discussion

Developed with clues from experiments, the theory draws from several branches of physical chemistry and condensed matter physics. It describes the charging process as proceeding in three stages: growth before collision, impact, and separation.

Each of the stages involves fundamental processes, some of which are still incompletely known, so that approximations are necessary, but a quantitative description of a recent study of ice-ice collisions is achieved with only one adjustable constant. Application to most collisional charging studies, whereby a rimed target is impacted by small ice particles, is not as detailed. These experiments are designed to represent the typical charging conditions in thunderstorms and are therefore the testing grounds for the natural phenomenon. Quantitative applications of the theory to atmospheric conditions may be even more limited because of the difficulty in characterizing the surfaces, collisions, and environments.

The qualitative aspects of the mass and charge exchange are as follows: (1) The more rapidly a particle is growing, the greater its surface density of negative ions. (2) Collisions produce melting at the surface of both particles, which liberates the surface ions into the liquid, where they diffuse rapidly to uniform number density. (3) When the two particles separate, they take roughly equal portions of the liquid. (4) Thus the more rapidly growing particle, having lost more negative ions, becomes positively charged. (5) Melting may not be equal on the two surfaces; in the

MD experiment the growing particle is colder and therefore its melting is somewhat less. On separation it receives a net increase of mass, which brings some negative charge back to it, but since it is a small fraction of the total melt, it does not eliminate the net loss of negative charge. (6) Saturation of this process occurs as the growth rate, and hence negative surface charge density and local electric field, increases and localizes neutralizing counterions.

In order to apply the charge transfer theory to atmospheric phenomena, we have made several essential simplifications. The state of the graupel surface is rough and disordered by rapid vapor growth and riming, and yet the calculation of collisional contact area tacitly assumes the surface as smooth. The same assumption was made by *Gaskell and Illingworth* [1980], in applying the same relation as (14), to ice-graupel collisions. The simplification may be justified for those collisions that cause melting deeper than the depth of surface roughness or where the size of the impacting particle is greater than the lateral scale of surface roughness. Additional complications, involving a detailed examination of the different types of collisions, would go beyond the scope and intention of this paper. However, it is hoped that future experimental studies will help to elaborate the model to make it suitable for useful practical applications.

Acknowledgments. We are grateful for discussions with M.B. Baker, M.Den Nijs, S.C. Fain, R. Jayaratne, and H. Jónsson. This work is supported by the Leonard X. Bosack and Bette M. Kruger Charitable Foundation and by the National Science Foundation.

References

Arakawa, M., and M. Higa, Measurements of ejection velocities in collisional disruption of ice spheres, *Planet. Space Sci., 44*, 901–980, 1996.

Avila, E. E., G. G. Aquirre Varela, and G. M. Caranti, Charging in ice-ice collisions as a function of the ambient temperature and the larger particle average temperature, *J. Geophys. Res., 101*, 29,609–29,614, 1996.

Baker, B., M. B. Baker, E. R. Jayaratne, J. Latham, and C.~P.~R. Saunders, The influence of diffusional growth rates on the charge transfer accompanying rebounding collisions between ice crystals and soft hailstones, *Q. J. R. Meteorol. Soc., 113*, 1193–1215, 1987.

Baker, M. B., and J. G. Dash, Charge transfer in thunderstorms and the surface melting of ice, *J. Cryst. Growth, 97*,770–776, 1989.

Baker, M. B., and J. G. Dash, Mechanism of charge transfer between colliding ice particles in thunderstorms, *J. Geophys. Res., 99*, 10,621–10,626, 1994.

Beaglehole, D., and D. Nason, Transition layer on the surface of ice, *Surf. Sci., 96*, 357–363, 1980.

Beaglehole, D., and P. Wilson, Extrinsic premelting at the ice-glass interface, *J. Phys. Chem., 98*, 8096–8100, 1994.

Brooks, I. M., C. P. R. Saunders, R. P. Mitzeva, and S. L. Peck, The effect on thunderstorm charging of the rate of rime accretion by graupel, *Atmos. Res., 43*, 277–295, 1997.

Buser, O., and A. N. Aufdermaur, Electrification by collisions of ice particles on ice or metal targets, in *Electrical Processes in Atmospheres*, edited by H. Dolezak and R. Reiter, pp. 294–301, Steinkopf, Darmstadt, Germany, 1977.

Caranti, J. M., and A. J. Illingworth, The contact potential of rimed ice, *J. Phys. Chem., 87*, 4125–4130, 1983.

Caranti, G. M., E. E. Avila, and M. A. Re, Charge transfer during individual collisions in ice growing from vapor deposition, *J. Geophys. Res., 96*, 15,365–15,375, 1991.

Dash, J. G., H.-Y. Fu, and J. S. Wettlaufer, The premelting of ice and its environmental consequences, *Rep. Prog. Phys., 58*, 115–167, 1995.

Dosch, H., A. Lied, and J. H. Bilgram, Glancing-angle x-ray scattering studies of the premelting of ice surfaces, *Surf. Sci., 327*, 145–164, 1995.

Dosch H., A. Lied, and J. H. Bilgram, Disruption of the hydrogen-bonding network at thesurface of Ih ice near surface premelting, *Surf. Sci., 366*, 43–50, 1996.

Eigen, M., and L. De Maeyer, Self-dissociation and protonic charge transport in water and ice, *Proc. R. Soc. London, Ser. A, 247*, 505–533, 1958.

Einstein, A., On the movement of small particles suspended in a stationary liquid demanded by the molecular-kinetic theory of heat, in *Investigations on the Theory of Brownian Movement*, pp. 1–18, Dover, Miheola, N.Y., 1905.

Elbaum, M., S. G. Lipson, and J. G. Dash, Optical study of surface melting on ice, *J. Cryst. Growth, 129*, 491–505, 1993.

Engelhardt, H., Protonic conduction in ice, in *Physics and Chemistry of Ice*, edited by E. Whalley, S. J. Jones, and L. W. Gold, pp. 226–235, Royal Soc. of Can., Ottawa, 1973.

Fletcher, N. H., *The Chemical Physics of Ice*, Cambridge Univ. Press, New York, 1970.

Frenken, J. W. M., and H. M. van Pinxteren, Surface melting: Dry, slippery, wet and faceted surfaces, *Surf. Sci., 307–309*, 728-734, 1994.

Furukawa, Y., M. Yamamoto, and T. Kuroda, Ellipsometric study of the transition layer on the surface of an ice crystal, *J. Cryst. Growth, 82*, 665–677, 1987.

Gaskell, W., and A. J. Illingworth, Charge transfer accompanying individual collisions between ice particles and its role in thunderstorm electrification, *Q. J. R. Meteorol. Soc., 106*, 841–854, 1980.

Israelachvili, J. N., *Intermolecular and Surface Forces*, chap. 12, Academic, San Diego, California, 1992.

Jayaratne, E. R., Density and surface temperature of graupel and the charge separation during ice crystal interactions, *J. Geophys. Res., 103*, 13,957–13,961, 1998.

Jayaratne, E. R., C. P. R. Saunders, and J. Hallett, Laboratory studies of the charging of soft-hail during ice crystal interactions, *Q. J. R. Meteorol. Soc., 109*, 609–630, 1983.

Jayaratne, E. R., S. L. Peck, and C. P. R. Saunders, Comments on "A laboratory study of static charging by fracture in ice growing by riming," by Avila and Caranti, *J. Geophys. Res., 101*, 9533–9535, 1996.

Keith, W. D., and C. P. R. Saunders, Further laboratory studies of the charging of graupel during ice crystal interactions, *Atmos. Res., 25*, 445–464, 1990.

Kouchi, A., T. Yamamoto, T. Kozasa, T. Kuroda, and J. M. Greenberg, Conditions for condensation and preservation of amorphous ice and crystallinity of astrophysical ices, *Astron. Astrophys., 290*, 1009–1018, 1994.

Krim, J., and G. Palasantzas, Experimental observations of self-affine scaling and kinetic roughening at sub-micron length scales, *Int. J. Mod. Phys., 9*, 599–632, 1995.

Latham, J., and C. D. Stow, The influence of impact velocity and ice specimen geometry of the charge transfer associated with temperature gradients in ice, *Q. J. R. Meteorol. Soc., 91*, 462–470, 1965.

Löwen, H., Melting, freezing and colloidal suspensions, *Phys. Rep., 237*, 249–324, 1994.

Mae, S., and A. Higashi, Effects of plastic deformation on the dielectric properties of ice (H_3O^+ mobility and dislocation generation), *Cryst. Lattice Defects, 4*, 295–308, 1973.

Mason, B. L., and J. G. Dash, Surface melting of ice and thunderstorm electrification, in *Ice Physics in the Natural Environment, NATO ASI, Ser. I*, vol. 56, edited by J. S. Wettlaufer, J. G. Dash, and N. Untersteiner, pp. 321–324, Springer-Verlag, New York, 1999.

Mason, B. L., and J. G. Dash, Charge and mass transfer in ice-ice collisions: Experimental observations of a mechanism in thunderstorm electrification, *J. Geophys. Res., 105*, 10,185–10,192, 2000.

Mizuno, V., and N. Hanafusa, Studies of surface properties of ice using nuclear magnetic resonance, *J. Phys. Collog., C1, 48, suppl. 3*, 511–516, 1987.

Nenow, D., and A. Trayanov, Surface premelting phenomena, *Surf. Sci., 213*. 488–501. 1989.

Netz, R. R., and D. Andelman, Roughness-induced wetting, *Phys. Rev. E, 55*, 687–700, 1997.

Onsager, L., and M. Dupuis, The electrical properties of ice, *Proc. Int. Sch. Enrico Fermi, X*, 294–315, 1959.

Oxtoby, D., Nucleation and surface melting of ice, in *Ice Physics in the Natural Environment, NATO ASI, Ser. I*, vol. 56, edited by J. S. Wettlaufer, J. G. Dash, and N. Untersteiner, pp. 23–38, Springer-Verlag, New York, 1999.

Pengra, D. B., D.-M. Zhu, and J. G. Dash, Surface melting of strained and unstrained layers: Kr, Ar, and Ne, *Surf. Sci., 245*, 125–131, 1991.

Pines, E., and D. Huppert, Kinetics of proton transfer in ice via the pH-

jump method: Evaluation of the proton diffusion rate in polycrystalline doped ice, *Chem. Phys. Lett., 116*, 295–301, 1985.

Pittenger, B., D. J. Cook, C. R. Slaughterbeck, and S. C. Fain Jr., Investigation of ice-solid interfaces by force microscopy: Plastic flow and adhesive forces, *J. Vac. Sci. Technol. A, 16*(3), 1832–1837, 1998.

Qian, J., and C. K. Law, Regimes of coalescence and separation in droplet collision, *J. Fluid Mech., 331*, 59–80, 1997.

Reynolds, S. E., M. Brook, and M. F. Gourley, Thunderstorm charge separation, *J. Meteorol., 14*, 426–436, 1957.

Saunders, C. P. R., Thunderstorm electrification laboratory experiments and charging mechanisms, *J. Geophys. Res., 99*, 10,773–10,779, 1994.

Saunders, C. P. R., and S. L. Peck, Laboratory studies of the influence of the rime accretion rate on charge transfer during crystal/graupel collisions, *J. Geophys. Res., 103*, 13,949–13,961 1998.

Saunders, C. P. R., W. D. Keith, and R. P. Mitzeva, The effect of liquid water on thunderstorm charging, *J. Geophys. Res., 96*, 11,007–11,017, 1991.

Smith, R. W., and D. J. Srolovitz, Void formation during film growth: A molecular dynamics simulation study, *J. Appl. Phys., 79*, 1448–1457, 1996.

Stolze, P., and J. K. Norskov, Accommodation and diffusion of Cu deposited on flat and stepped Cu(111) surfaces, *Phys. Rev. B, 48*, 5607–5611, 1993.

Tabor, D., *The Hardness of Metals*, Clarendon, Oxford, England, 1951.

Takahashi, T., Electric potential of a rubbed ice surface, *J. Atmos. Sci., 26*, 1259–1265, 1969.

Takahashi, T., Riming electrification as a charge generation mechanism in thunderstorms, *J. Atmos. Sci., 35*, 1536–1548, 1978.

Verwey, E. J. W., and J. T. G. Overbeek, *Theory of Stability of Lyophobic Colloids*, Elsevier, New York, 1948.

Wettlaufer, J. S., Impurity effects in the premelting of ice, *Phys. Rev. Lett., 82*, 2516–2519, 1999.

Wettlaufer, J. S., M. G. Worster, L. A. Wilen, and J. G. Dash, A theory of premelting dynamics for all power law forces, *Phys. Rev. Lett., 76*, 3602–3605, 1996.

Zhu, D.-M., and J. G. Dash, Surface melting in argon and neon, *Phys. Rev. Lett., 57*, 2959–2962, 1986.

J. D. Dash, Department of Physics, University of Washington, Box 351560, Seattle, 98195. (dash@phys.washington.edu)

B. L. Mason, Stanford Research Systems, 1290 D Reamwood Avenue, Sunnyvale, CA 94089.

J. S. Wettlaufer, Applied Physics Laboratory, University of Washington, 1013 N.E. 40th Street, Seattle, 98105. (wett@apl.washington.edu)

(Received March 31, 2000; revised August 28, 2000;
accepted January 30, 2001.)